

Absorption and opacity threshold for a thin foil in a strong laser field

E.G. Gelfer,^{1,2,*} A.M. Fedotov,² O. Klimo,^{1,3} and S. Weber¹

¹*ELI Beamlines, Institute of Physics of the ASCR,
v.v.i., Dolni Brezany, Czech Republic*

²*National Research Nuclear University “MEPhI”, Moscow, Russia*

³*FNSPE, Czech Technical University in Prague, Czech Republic*

Abstract

According to simulations, a commonly accepted threshold for a transition from transparency to opaqueness of a thin foil interacting with a strong circularly polarized laser pulse needs a refinement. Here we reestablish such a threshold condition by properly taking into account the dominance of laser absorption. Our model is confirmed by PIC simulations and predicts that the threshold value is less sensitive to the laser pulse amplitude than assumed previously. Interaction with an opaque foil leads to a steepening of the laser pulse front, and this can be important for applications.

INTRODUCTION

A key attribute specifying the laser-matter interaction regime is transparency or opacity of a target to an incident laser pulse [1, 2]. Precise formulation of a relevant discriminating criterion is crucially important for many modern applications, including laser contrast enhancement by plasma shutters [3, 4], laser frequency upshift by relativistic electron mirrors [5], plasma based polarizers [6], generation of gamma-rays [7, 8] and bright neutron bunches [9] in laser plasmas, as well as for laser plasma ion acceleration [10–15]. The latter can be applied for a wide range of purposes (see the review [16]) from fast ignition in fusion targets [17] to cancer treatment [18]. As radiation pressure acceleration of ions is most efficient when the target density is kept slightly above the threshold [11, 16], it is reasonable to optimize the laser pulse temporal profile to maintain such a condition as long as possible [19]. In contrast, transparent targets are preferable for observation and detailed studies of an impact of radiation friction on plasma dynamics [20–22] or strong field QED effects [23], as otherwise fewer electrons can ever reach the focal region to probe the strongest field. Such studies are planned with the next generation laser facilities under construction [24–27].

As is well known [28], a moderately intense laser pulse (of dimensionless field strength $a_0 \equiv eE_0/m\omega c \lesssim 1$) can penetrate through a thick plasma target (of thickness $d \gg \lambda$, where λ is the laser carrier wavelength) only if the unperturbed target density n_0 is less than the critical value $n_{cr} = m\omega^2/4\pi e^2$. Here E_0 is the electric field strength amplitude, ω is the laser carrier frequency, m and $-e$ are electron mass and charge. For a strong pulse, $a_0 \gg 1$, this condition is modified to $n_0 \lesssim a_0 n_c$ [29, 30] due to the effect of relativistic self-induced transparency (RSIT), see also the discussion on the elaboration of this criterion in [31–35].

Here we study the opposite case of a thin foil target ($d \lesssim \lambda$), assuming that the laser pulse has ultrarelativistic intensity ($a_0 \gg 1$), is circularly polarized and is incident normally. For such a case the transparency threshold condition obtained in [36] (see also [13]) involves the dimensionless electron areal density $\sigma_0 = (n_0/n_{cr}) \cdot (\omega d/c)$ of the foil and can be cast to the form

$$\sigma_0 < \sigma_0^{th} = 2a_0. \quad (1)$$

However, according to the results of PIC simulations, the threshold value in Eq. (1) needs a refinement if a_0 is a few hundred or higher. For example, a foil with $\sigma_0 \approx 88$ can still remain opaque to a laser pulse even for $a_0 = 500$ (see Fig. 1a), i.e. for more than an order

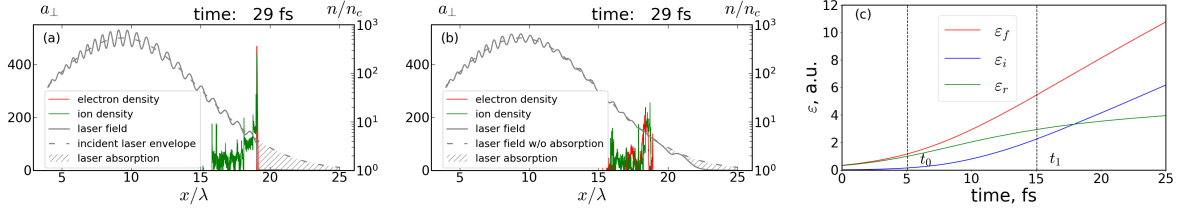


FIG. 1: 1D PIC simulation results for the interaction of a strong circularly polarized Gaussian laser pulse ($\lambda = 1\mu\text{m}$, $a_0 = 500$, FWHM duration 30fs) with a thin hydrogen foil (thickness $d = 0.1\lambda$). (a): foil electron density $n_0 = 140n_c$ (areal density $\sigma_0 \approx 88$) – the foil is opaque; (b): foil electron density $n_0 = 80n_c$ (areal density $\sigma_0 \approx 50$) – the foil is transparent; (c): time dependencies of the laser front (hatched in Fig.1a) energy (ϵ_f), the ions energy (ϵ_i) and the reflected energy (ϵ_r) for $n_0 = 140n_c$.

of magnitude higher value than prescribed by the threshold (1). The reason is that in a derivation of the condition (1) it is assumed that laser absorption is negligible so that an incident laser pulse is totally reflected by an opaque target. But it turns out that for high enough values of a_0 the absorption can become crucially important, thus setting up a lower areal density limit for RSIT, which then depends more on a laser pulse duration and envelop shape than on its amplitude.

1D MODEL

Let us illuminate the role of laser absorption using a 1D laser–foil interaction model with a due consideration of the laser pulse temporal profile. Denote by $a(t)$ the value of the dimensionless laser field strength at time t at the foil position x_t . Upon the incidence of a laser pulse on a foil $a(t)$ is gradually growing from zero onward. Let t_0 be the least moment when $a(t_0) = \sigma_0/2$. Then, according to Eq. (1), while $t < t_0$ the laser pulse front is totally reflected by the foil, as shown in Fig. 1 (c). Hence the field behind the foil vanishes, $\mathbf{E}(t, x > x_t) = 0$, and the laser profile eventually takes a step-like form similar to the one shown in Fig. 1 (a). Such a profile creates a strong longitudinal ponderomotive force, which efficiently accelerates the electrons forward. Electrons in turn pull the ions behind themselves, therefore the whole plasma gets accelerated in front of the laser pulse. For $t > t_0$ the reflection saturates and, assuming that transition to transparency is procrastinated, upon

the further growth of $a(t)$ the rest of the pulse bulk is being absorbed. The absorbed energy is eventually transferred to the ions, thus enforcing their acceleration. We are especially interested in an initial stage of the process when the ions still remain mildly relativistic. To refine the threshold, it is enough to thoroughly balance the energies absorbed from the laser pulse and gained by the ions (here the energy gained by electrons can be neglected as is much smaller).

Initially, as long as the ions are slow, $v_i \ll c$, they lag behind the electrons, hence do not overlap with them and the dimensionless charge separation field can be estimated as σ_0 . At this stage the longitudinal component of the ions 4-velocity is $u_i \sim \mu Z n_{cr} \sigma_0 (\tau - \tau_0) / \omega A$, where A and Z are the ion mass and charge numbers, μ is the electron-to-proton mass ratio, $\tau = \omega t$, and from now on we assume the units are such that the speed of light $c = 1$. Importantly, it is taken into account that a large scale ion acceleration starts only together with laser absorption. The ions become mildly relativistic, $u_i \sim 1$, at $\tau = \tau_0 + \tau_1$, where

$$\tau_1 = \frac{A}{Z \mu \sigma_0} \quad (2)$$

is the required duration of their acceleration. The total energy of the ions at this moment can be estimated as

$$\varepsilon_i(\tau_1) \sim \frac{A n_{cr} \sigma_0}{Z \omega \mu} S m_e, \quad (3)$$

where S is the laser pulse cross section.

Next consider the energy of a part of the laser pulse front having touched the foil by the moment τ_1 (for the sake of clarity in Figs. 1 (a) and (b) an imaginary envelope for free propagation of the pulse in the absence of the target is plotted dashed and its corresponding part is hatched). For brevity, in what follows let us call it just the laser front energy. Let us write the initial envelope as $a(\varphi) = a_0 g(\varphi/T)$, where φ is the phase, T is the characteristic dimensionless duration and g is the dimensionless profile function of the order of unity decaying at $\varphi \gg 1$. Then the energy stored in the front of the laser pulse during $\tau_0 < \tau < \tau_0 + \tau_1$ can be estimated by

$$\varepsilon_f(\tau_1) \sim \frac{a_0^2 n_{cr} S}{\omega} m_e \int_{\tau_0}^{\tau_0 + \tau_1} g^2(\tau/T) d\tau. \quad (4)$$

If the foil remains opaque at $\tau \sim \tau_1$, then this energy should be eventually entirely absorbed by the ions and hence should be equal to (3), see Fig. 1 (c). The integral encountering in

Eq. (4) can be approximated as

$$\int_{X_0}^{X_0+X_1} f(\xi)d\xi \approx \frac{f^2(X_0)}{f'(X_0)} \left[e^{X_1 f'(X_0)/f(X_0)} - 1 \right], \quad \text{if } \left| \frac{f''(X_0)f(X_0)}{(f'(X_0))^2} - 1 \right| \ll 1. \quad (5)$$

Hence by equating (3) to (4) and taking into account that

$$a_0 g(\tau_0/T) = \sigma_0/2, \quad (6)$$

we arrive at

$$e^\zeta - 1 \approx 4\zeta, \quad (7)$$

where $\zeta = 2A|g'(\tau_0/T)|/(Z\mu\sigma_0 Tg(\tau_0/T))$.

Equation (7) has an approximate solution $\zeta \approx 2.3$, but this way the opacity threshold is slightly overestimated, since we did not take into account partial reflection of the laser pulse. In fact, as shown below, an almost perfect agreement with simulations can be obtained by taking $\zeta = 2.7$. So that the refined opacity threshold can be finally formulated in the form

$$\mu T \sigma_0 \frac{Z}{A} \frac{g(\tau_0/T)}{|g'(\tau_0/T)|} \approx 0.75, \quad (8)$$

where τ_0 is determined by (6). Note that our approximation (5) is valid only for $|\tau_0| \gg T$, i.e. for $\sigma_0 \ll a_0$ or $a_0 \gg A/TZ\mu$, as otherwise reflection dominates over the absorption and the usual transparency condition Eq. (1) remains valid. It is also worth to emphasize that our approach is reasonable only for circularly polarized pulses as otherwise a double layer consisting of an electron spike followed by the ions [see Fig. 1 (a)] is rapidly messed up due to electron heating [37, 38].

In order to compare Eq. (8) with numerical simulations, let us specify it more explicitly for the two particular examples of Gaussian and linear profiles. Namely, if the function $g(\xi)$ is Gaussian, $g(\xi) = e^{-\xi^2}$, then the threshold areal density σ_{th}^G is determined by

$$\frac{\sigma_{th}^G}{\sqrt{\ln(2a_0/\sigma_{th}^G)}} \approx 1.5 \frac{A}{TZ\mu}. \quad (9)$$

Note that the refined threshold depends on the laser field amplitude a_0 much weaker than on the remaining parameters (pulse duration or on ion mass and charge numbers). For our second example of a linear profile [$g(\xi) = 0$ for $\xi < 0$, $g(\xi) = \xi$ for $0 < \xi < 1$, and $g(\xi) = 1$ for $\xi > 1$] the approximation (5) is invalid, but the integral in (4) is easily evaluated directly, so that instead of (8) we arrive at

$$\sigma_{th}^L \approx \sqrt{\frac{1.5a_0}{T} \frac{A}{Z\mu}}. \quad (10)$$

One can observe that here the refined threshold is fully determined by the envelope slope rather than by laser pulse amplitude or duration separately.

The obtained above estimations for the areal threshold densities [see Eqs. (9) – (10)] are compared to the values obtained by 1D PIC simulations in Fig. 2. Namely we performed a set of simulations for several values of pulse duration and for three types of ions: hydrogen ($Z/A = 1$), deuterium ($Z/A = 0.5$) and tritium ($Z/A = 0.33$). Field strength amplitude was fixed ($a_0 = 500$), but for a Gaussian pulse we have checked that the results remained almost unchanged if a_0 was increased up to 1000 and 1500. We used targets with a fixed thickness $d = 0.1\lambda$ but varying density. One can observe a perfect agreement between the theory and simulations, though, as expected, the simulation results start to deviate from the model when σ_{th} is so high that approaches a_0 .

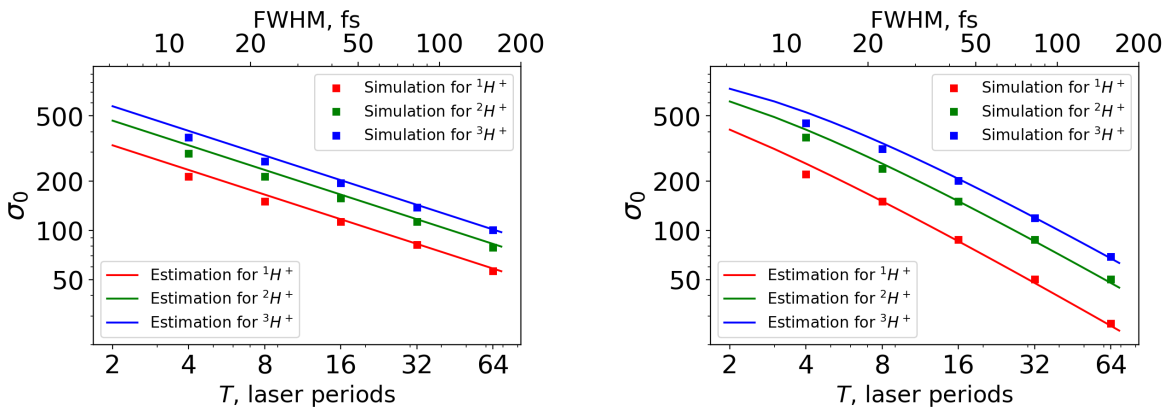


FIG. 2: Estimations vs 1D PIC simulation results for transparency threshold areal density for different pulse durations and ion charge-to-mass ratios. Dimensionless field amplitude $a_0 = 500$, laser carrier wavelength $\lambda = 1\mu\text{m}$, foil thickness $d = 0.1\lambda$. Left panel: linear pulse profile, right panel: Gaussian pulse profile.

2D SIMULATIONS

The main additional effect arising in a 2D case is the Rayleigh-Taylor instability (RTI) of a thin foil irradiated by a strong laser pulse. In the case of relativistic motion of the foil its growth time is [39]

$$\tau_{RT} \sim \sqrt{\frac{\mu\sigma_0}{A}} \frac{1}{k^{3/2}}, \quad (11)$$

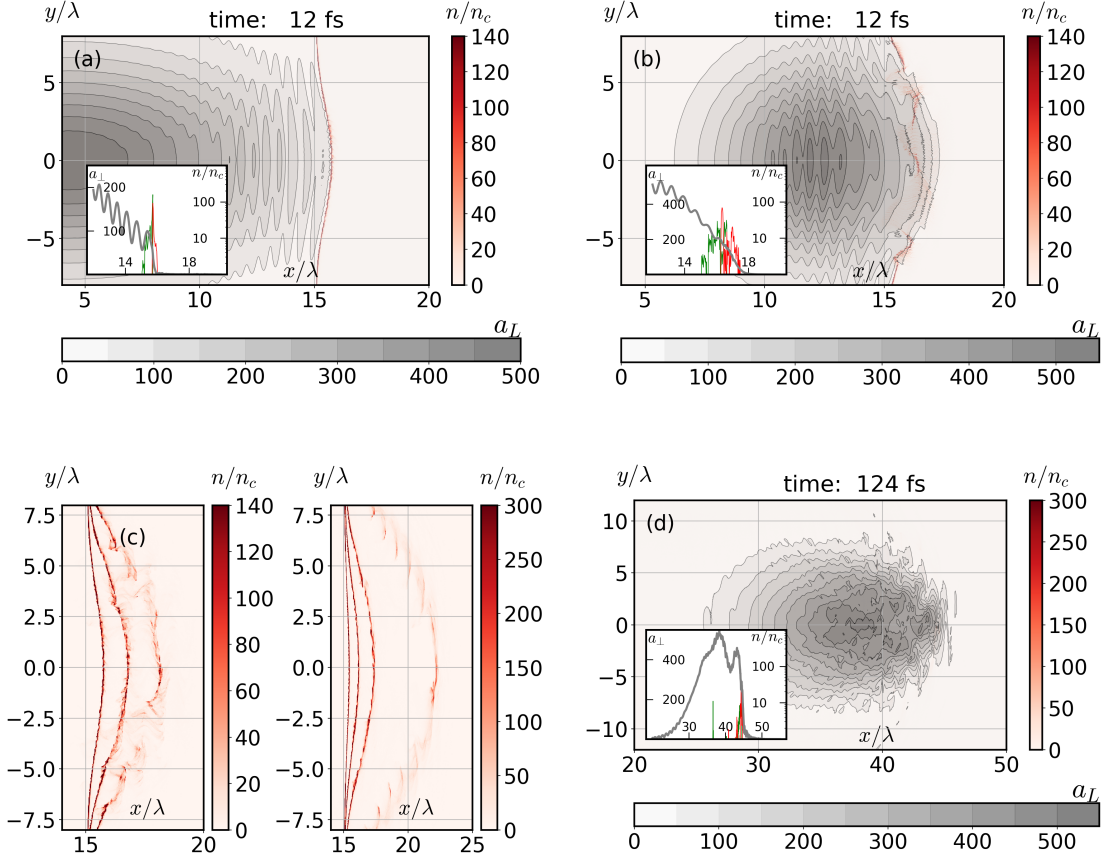


FIG. 3: 2D PIC simulation results. $a_0 = 500$, transverse waist radius $w = 6\lambda$, $\lambda = 1\mu m$, $d = 0.1\lambda$, H^+ ions. (a), (b), (d): electron (red), ion (green) densities and laser field (grey) distributions for laser pulse FWHM 30 fs [(a) and (d)] and 15 fs [(b)], target density $n_0 = 140n_c$ [(a) and (b)] and $n_0 = 300n_c$ [(d)]; insets: a sectional view at $y = 0$. (c): electron density distributions at subsequent moments of time for different target densities. Left: $n_0 = 140n_c$ and $t = 12$ fs, 18 fs, 26 fs; right: $n_0 = 300n_c$ and $t = 12$ fs, 18 fs, 26 fs, 46 fs.

where k is the dimensionless wave vector of a perturbation and Eq. (6) is taken into account.

To check reliability of our estimations in 2D we performed 2D PIC simulations for a pulse with Gaussian profiles in both longitudinal and transverse directions (see Fig. 3). It turns out that our estimate (9) for the transparency threshold areal density still remains valid. This can be confirmed by comparing Figs 3 (a) and (b), where the interaction of laser pulses of different durations but of the same amplitude with identical targets is displayed. The duration of the laser pulse in Fig. 3 (a) according to the condition (9) corresponds to opacity, while the pulse in Fig. 3 (b) is taken twice shorter, resulting in target transparency.

At later times RTI distorts the target and eventually destroys it, see Fig. 3 (c), therefore it is meaningless to discuss its transparency for times $t \gg \tau_{RT}$. However, since τ_{RT} is proportional to $\sqrt{\sigma_0}$, denser targets survive under RTI longer, see Fig. 3 (c). Besides, similarly to the 1D case, target opaqueness leads to the steepening of a laser front, see Fig. 3 (d), and after the destruction of the target the resulting steepened pulse with an increased femtosecond level contrast can be used for applications [3, 4, 40, 41].

CONCLUSION

To conclude, we have demonstrated that a commonly accepted threshold for opaqueness of a thin foil to a strong circularly polarized laser pulse needs a revision. It is shown that such a refinement is due to laser absorption not properly taken into account in previous studies. As a consequence, with shorter laser pulses RSIT can be achieved for smaller areal density of a target. Interestingly, it turns out that for Gaussian pulses the refined threshold areal density is almost independent of the field amplitude, depending only on pulse duration and the ions charge-to-mass ratio. Our findings are in excellent agreement with 1D PIC simulations. They are in agreement with 2D simulations as well, though in a 2D case the effect is strongly distorted by the Rayleigh-Taylor instability.

Moreover, if a front part of the pulse gets totally absorbed like in Fig. 1 (a), then the target acts as a plasma shutter [3, 4, 40, 41] steepening the pulse front and increasing laser contrast on a femtosecond level. This can be important for a wide range of applications, including high harmonic generation [42, 43] and laser ion acceleration. In the latter case high contrast enhances the energy [44] and suppresses the divergence [45, 46] of the accelerated ion beams, it is also crucial for such highly efficient ion acceleration mechanisms as radiation pressure acceleration [11, 47] and breakout afterburner [14]. Though the effect reported here reveals in thick targets as well, see e.g. [35], its proper description in such a case requires further studies.

ACKNOWLEDGMENTS

We are grateful to M. Grech and Y.J. Gu for valuable discussions. The results of the project LQ1606 were obtained with the financial support of the Ministry of Edu-

cation, Youth and Sports of the Czech Republic as part of targeted support from the National Programme of Sustainability II. The research was performed using the code SMILEI [48] and the resources of the ELI Beamlines Eclipse cluster, and was partially supported by the MEPHI Academic Excellence Project (Contract No. 02.a03.21.0005), Russian Foundation for Basic Research (Grant 19-02-00643), Czech Science Foundation Project No. 18-09560S, projects ELITAS (ELI Tools for Advanced Simulation) CZ.02.1.01/0.0/0.0/16_013/0001793, ADONIS (Advanced research using high intensity laser produced photons and particles) CZ.02.1.01/0.0/0.0/16_019/0000789 and HiFI (High-Field Initiative) CZ.02.1.01/0.0/0.0/15003/0000449 from European Regional Development Fund.

* Electronic address: egelfer@gmail.com

- [1] G. A. Mourou, T. Tajima, and S. V. Bulanov, *Rev. Mod. Phys.* **78**, 309 (2006).
- [2] A. Macchi, *A Superintense Laser-Plasma Interaction Theory Primer* (Springer, 2013).
- [3] S. A. Reed, T. Matsuoka, S. Bulanov, M. Tampo, V. Chvykov, G. Kalintchenko, P. Rousseau, V. Yanovsky, R. Kodama, D. W. Litzenberg *et. al.*, *Appl. Phys. Lett.* **94**, 201117 (2009).
- [4] S. Palaniyappan, B. M. Hegelich, H.-C. Wu, D. Jung, D. C. Gautier, L. Yin, B. J. Albright, R. P. Johnson, T. Shimada, S. Letzring *et. al.*, *Nature Physics* **8**, 763-769 (2012).
- [5] D. Kiefer, M. Yeung, T. Dzelzainis, P. S. Foster, S. G. Rykovanov, C. L. S. Lewis, R. S. Marjoribanks, H. Ruhl, D. Habs, J. Schreiber *et. al.*, *Nat. Comms.* **4**, 1763 (2013).
- [6] D. J. Stark, C. Bhattacharjee, A. V. Arefiev, T. Toncian, R. D. Hazeltine, and S. M. Mahajan, *Phys. Rev. Lett.* **115**, 025002 (2015).
- [7] C. S. Brady, C. P. Ridgers, T. D. Arber, and A. R. Bell, *Phys. Plasmas* **21**, 033108 (2014).
- [8] H. X. Chang, B. Qiao, Y. X. Zhang, Z. Xu, W. P. Yao, C. T. Zhou, and X. T. He, *Phys. Plasmas* **24**, 043111 (2017).
- [9] M. Roth, D. Jung, K. Falk, N. Guler, O. Deppert, M. Devlin, A. Favalli, J. Fernandez, D. Gautier, M. Geissel *et. al.* *Phys. Rev. Lett.* **110**, 044802 (2013).
- [10] S. C. Wilks, W. L. Kruer, M. Tabak and A. B. Langdon, *Phys. Rev. Lett.* **69**, 1383 (1992).
- [11] T. Esirkepov, M. Borghesi, S. V. Bulanov, G. Mourou and T. Tajima, *Phys. Rev. Lett.* **92**, 175003 (2004).

- [12] B. Qiao, M. Zepf, M. Borghesi and M. Geissler, Phys. Rev. Lett. **102** 145002 (2009).
- [13] A. Macchi, S. Veghini and F. Pegoraro, Phys. Rev. Lett. **103**, 085003 (2009); A. Macchi, S. Veghini, T. V. Liseykina and F. Pegoraro, New J. Phys. **12**, 045013 (2010).
- [14] L. Yin, B. J. Albright, K. J. Bowers, D. Jung, J. C. Fernandez, and B. M. Hegelich Phys. Rev. Lett. **107**, 045003 (2011).
- [15] S. S. Bulanov, E. Esarey, C. B. Schroeder, S. V. Bulanov, T. Zh. Esirkepov, M. Kando, F. Pegoraro and W. P. Leemans, Phys. Rev. Lett. **114**, 105003 (2015).
- [16] A. Macchi, M. Borghesi, and M. Passoni, Rev. Mod. Phys. **85**, 751 (2013).
- [17] N. Naumova, T. Schlegel, V. T. Tikhonchuk, C. Labaune, I. V. Sokolov and G. Mourou, Phys. Rev. Lett. **102**, 025002 (2009).
- [18] S. V. Bulanov, T. Z. Esirkepov, V. S. Khoroshkov, A. V. Kunetsov, and F. Pegoraro, Phys. Lett. A **299**, 240 (2002).
- [19] S. S. Bulanov, C. B. Schroeder, E. Esarey, and W. P. Leemans, Phys. Plasmas **19**, 093112 (2012).
- [20] M. Tamburini, F. Pegoraro, A. Di Piazza, C. H. Keitel, and A. Macchi New J. Phys. **12**, 123005 (2010).
- [21] A. Gonoskov, A. Bashinov, I. Gonoskov, C. Harvey, A. Ilderton, A. Kim, M. Marklund, G. Mourou, and A. Sergeev, Phys. Rev. Lett. **113**, 014801 (2014); L. L. Ji, A. Pukhov, I. Yu. Kostyukov, B. F. Shen, and K. Akli, Phys. Rev. Lett. **112**, 145003 (2014); A. M. Fedotov, N. V. Elkina, E. G. Gelfer, N. B. Narozhny, and H. Ruhl, Phys. Rev. A **90**, 053847 (2014).
- [22] E. Gelfer, N. Elkina, A. Fedotov, Sci. Rep. **8**, 6478 (2018); E. G. Gelfer, A. M. Fedotov, S. Weber, PPCF **60**, 064005 (2018).
- [23] A. Di Piazza, C. Muller, K. Z. Hatsagortsyan, and C. H. Keitel C.H., Rev. Mod. Phys. **84**, 1177 (2012).
- [24] <http://www.eli-beams.eu>
- [25] <http://www.eli-np.ro/>
- [26] <http://portail.polytechnique.edu/luli/en/cilex-apollon/apollon>
- [27] Z. Guo, L. Yu, J. Wang, C. Wang, Y. Liu, Z. Gan, W. Li, Y. Leng, X. Liang, R. Li, Optics Express, **26**, 26776–26786 (2018).
- [28] F. Chen, *Introduction to Plasma Physics and Controlled Fusion* (Springer US, 1984) Volume 1: Plasma Physics.

- [29] A. I. Akhiezer and R. V. Polovin, *Sov. Phys. JETP* **3**, 696–705 (1956).
- [30] P. Kaw and J. Dawson, *Phys. Fluids* **13**, 472 (1970).
- [31] F. Cattani, A. Kim, D. Anderson, and M. Lisak, *Phys. Rev. E* **62**, 1234 (2000).
- [32] V. V. Goloviznin and T. J. Schep, *Phys. Plasmas* **7**, 1564 (2000).
- [33] E. Siminos, M. Grech, S. Skupin, T. Schlegel, and V. T. Tikhonchuk *Phys. Rev. E* **86**, 056404 (2012).
- [34] E. Siminos, M. Grech, B. Svedung Wettervik, T Fülöp, *New J. Phys.* **19** 123042 (2017).
- [35] L. Ji, B. Shen, X. Zhang, *New J. Phys.* **20**, 053043 (2018).
- [36] V. A. Vshivkov, N. M. Naumova, F. Pegoraro, and S. V. Bulanov, *Phys. Plasmas* **5**, 2727 (1998).
- [37] A. Macchi, F. Cattani, T. V. Liseykina, F. Cornolti, *Phys. Rev. Lett.* **94**, 165003 (2005).
- [38] O. Klimo, J. Psikal, J. Limpouch, V.T. Tikhonchuk, *Phys. Rev. STAB* **11**, 031301 (2008).
- [39] F. Pegoraro and S. V. Bulanov, *Phys. Rev. Lett* **99**, 065002 (2007).
- [40] H. Y. Wang, C. Lin, Z. M. Sheng, B. Liu, S. Zhao, Z. Y. Guo, Y. R. Lu, X. T. He, J. E. Chen, and X. Q. Yan, *Phys. Rev. Lett.* **107**, 265002 (2011).
- [41] W. Q. Wei, X. H. Yuan, Y. Fang, Z. Y. Ge, X. L. Ge, S. Yang, Y. F. Li, G. Q. Liao, Z. Zhang, F. Liu *et. al.*, *Phys. Plasmas* **24**, 113111 (2017).
- [42] C. Thauray, F. Quere, J.-P. Geindre, A. Levy, T. Ceccotti, P. Monot, M. Bougeard, F. Reau, P. dOliveira, P. Audebert, R. Marjoribanks, Ph. Martin, *Nat. Phys.* **3**, 424 – 429 (2007).
- [43] M. Behmke, D. an der Brügge, C. Rödel, M. Cerchez, D. Hemmers, M. Heyer, O. Jckel, M. Kbel, G. G. Paulus, G. Pretzler *et. al.* *Phys. Rev. Lett.* **106**, 185002 (2011).
- [44] T. Ceccotti, A. Levy, H. Popescu, F. Reau, P. DOliveira, P. Monot, J. P. Geindre, E. Lefebvre, and Ph. Martin *Phys. Rev. Lett.* **99**, 185002 (2007).
- [45] J. S. Green, N. P. Dover, M. Borghesi, C. M. Brenner, F. H. Cameron, D. C. Carroll, P. S. Foster, P. Gallegos, G. Gregori, P. McKenna *et. al.*, *Plasma Phys. Controlled Fusion* **56**, 084001 (2014).
- [46] Y. Fang, X. L. Ge, S. Yang, W. Q. Wei, T. P. Yu, F. Liu, M. Chen, J. Q. Liu, X. H. Yuan, Z. M. Sheng, and J. Zhang, *Plasma Phys. Controlled Fusion* **58**, 075010 (2016).
- [47] A. P. L. Robinson, M. Zepf, S. Kar, R. G. Evans and C. Bellei, *New J. Phys.* **10** 013021 (2008).
- [48] J. Derouillat, A. Beck, F. Perez, T. Vinci, M. Chiaramello, A. Grassi, M. Fle, G. Bouchard,

I. Plotnikov, N. Aunai, J. Dargent, C. Riconda, M. Grech, *Comput. Phys. Commun.* **222**, 351–373 (2018).